Pergamon

Solar Energy, Vol. 54, No. 3, pp. 165–171, 1995

0038-092X/95 $9.50 + .00

0038-092X(94)00120-0

EFFECTS OF MISMATCH LOSSES IN PHOTOVOLTAIC ARRAYS

CHARLES E. CHAMBERLIN, PETER LEHMAN, JAMES ZOELLICK, AND GIAN PAULETTO
Environmental Resources Engineering, Humboldt State University, Arcata, CA 95521, U.S.A.

Abstract—Experimental and modeling results on the effects of mismatch losses in photovoltaic arrays are presented. Field tests conducted on each of the 192 modules are used to describe the variation in the properties of production run photovoltaic modules. Module specific estimates of a five-parameter module model are obtained by nonlinear regression. Mathematical models of four-module parallel string and series block photovoltaic array performance based on the five-parameter module model are developed and used to evaluate the variation in maximum output power and mismatch loss of arrays with random module orderings. Module maximum output power averaged 14% below the nameplate rating and exhibited a coefficient of variation of 2.1%. Mismatch losses were very small, never exceeding 0.53%. No differences between parallel string and series block arrays in array maximum output power were observed.

1. INTRODUCTION

In practical applications photovoltaic (PV) modules are wired together into electrical circuits or arrays to provide the necessary voltage and/or current. Bucciarelli (1979), Gonzalez and Weaver (1980), and others have noted that the performance of an array depends on the variability of the modules that comprise the array and the cells that comprise the modules. The difference between the maximum output power available from the array and the sum of the maximum output powers for each of the modules is referred to as the mismatch loss.

This article presents experimental and modeling results on the effects of mismatch losses in photovoltaic arrays. The variation in the current–voltage characteristics of production-run photovoltaic modules is described based on field tests conducted on 192 modules. After correction to normal operating cell temperature (NOCT) conditions of 1000 W m^{-2} and 47°C, the test results are used to estimate module-specific parameters of a five-parameter equivalent circuit model of the module. Mathematical models of the photovoltaic array performance based on the five-parameter module model are developed. Parallel string and series block array configurations are considered and the performance of these arrays with random module orderings is examined.

2. VARIATION IN MODULE PERFORMANCE

2.1 *Module testing*

Field performance tests were carried out on each of 192 ARCO Solar M75 Solar Electric Modules prior to installation in the photovoltaic array of the Schatz Solar Hydrogen Project at Humboldt State University. These modules contain single-crystal silicon cells and have nameplate ratings of 48 W at 1000 W m^{-2} insolation and 25°C cell temperature (STC) and 46.4 W at 1000 W m^{-2} insolation and 47°C cell temperature (NOCT). They were obtained as a single bulk purchase from the manufacturer and arrived in a single shipment.

The current–voltage characteristics or I–V curve for each module was measured under field conditions using a 0.1 F capacitive load and a 12-bit data acquisition system sampling at 100 hz. This testing system is described by Engle (1988). Each curve trace produced approximately 300 paired observations of module current and voltage. After sequential observations differing by less than 10 mA were removed to eliminate redundant observations, approximately 100 observation pairs remained for further analysis.

Insolation in the plane of the module was measured with an Eppley Precision Pyranometer PSP. Observed insolation during tests ranged from 760 to 1040 W m^{-2}. Module temperature was monitored using a Type E fast response, surface mounted thermocouple mounted at the center on the back of the module. Observed temperatures during tests ranged from 35 to 56°C.

Three of the 192 M75 modules were selected for a systematic investigation of the dependence of module current and voltage on measured insolation (E_m, W m^{-2}) and measured cell temperature (T_m, °C). I–V curves for each of these modules were measured at all combinations of five insolation levels from 800 to 1000 W m^{-2} and five cell temperature levels from 35 to 55°C. Open circuit voltage (V_{oc}, V) was found to depend on both T_m and E_m. Short circuit current (I_{sc}, A) was found to depend only on E_m. Based on these results, expressions to correct module current and voltage to NOCT were developed using multiple linear regression:

$$V = V_m \frac{V_{oc;r}}{V_{oc;m}} \quad (1)$$

where: V = module voltage corrected to NOCT (V);

Table 1. Quality of parameter estimates for module I–V curves at NOCT

Parameter	Units	Median estimate	Coefficient of variation of estimate (%)		
			Median	Minimum	Maximum
I_L	A	3.29	0.043	0.015	0.21
V_{OC}	V	18.20	0.040	0.018	0.22
R_S	Ω	0.32	4.1	0.075	11.0
R_P	Ω	160.0	3.8	0.062	11.0
ekt	V^{-1}	0.68	1.2	0.065	4.5

V_m = measured module voltage (V); $V_{oc;m}$ = measured module open circuit voltage (V); $V_{oc,r}$ = module open circuit voltage corrected to NOCT (V) = $V_{oc;m} + a(T_r - T_m) + b(E_r - E_m)$; a = temperature coefficient (V °C^{-1}); b = insolation coefficient (V m^2 W^{-1}); T_r = reference temperature (°C) = 47°C; and E_r = reference insolation (W m^{-2}) = 1000 W m^{-2}.

$$I = I_m \frac{E_r}{E_m} \tag{2}$$

where: I = module current corrected to NOCT (A), and I_m = measured module current (A).

2.2 *Module model*

The I–V curves of each module were described using a lumped equivalent circuit model developed by Lehman and Chamberlin (1987):

$$I = I_L - \left[\frac{I_L - \frac{V_{OC}}{R_P}}{\exp(ekt \cdot V_{OC}) - 1}\right] \times \{\exp[ekt(V + R_S I)] - 1\} - \frac{(V + R_S I)}{R_P} \tag{3}$$

or

$$I = f(V; I_L, V_{OC}, R_S, R_P, ekt) \tag{4}$$

where: I = module output current (A); V = module voltage (V); I_L = light induced module current (A); V_{OC} = open circuit module voltage (V); R_S = module series resistance (Ω); R_P = module parallel or shunt resistance (Ω); $ekt = \frac{q}{nkT}$ (V^{-1}); q = electron charge (C); n = dimensionless ideality factor; k = Boltzmann's constant (J °K^{-1}); and T = absolute cell temperature (°K).

The I–V curve for each module was characterized by module-specific values of five parameters: I_L, V_{OC}, R_S, R_P, and *ekt*. Note that this function is implicit with respect to I and requires solution by an iterative procedure such as Newton's method.

The five parameters were estimated by the Gauss–Newton method of least squares nonlinear regression using I as the dependent variable and V as the independent variable. The regression was carried out using NLPE, which is a general nonlinear regression program in FORTRAN developed by Bard (1967) and available in the public domain. The model fits the data well with standard deviations of the residuals of about 20 mA which is in the range of the discretization error associated with the analog-digital conversion. The parameter estimates for each module are statistically well-determined as shown in Table 1. I_L and V_{OC} are generally determined to within less than 0.1%. R_S, R_P, and *ekt* are generally determined to within 1–5%. Although correlations among the parameter estimates for R_S, R_P, and *ekt* were not zero and, therefore, unique parameter estimates cannot generally be obtained, it does not interfere with the accuracy of the estimated module I–V curves. Repeated tests on selected modules under different insolation and temperature conditions showed agreement in parameter estimates. Figure 1 shows the observed values of I and V along with the estimated I–V curve for a typical run.

2.3 *Model parameter distributions*

There was substantial variation in the I–V curve parameters among the 192 modules tested, as summarized in Table 2. R_S, R_P, and *ekt* exhibit the greatest variation from module to module with coefficients of variation of 33%, 48%, and 18%, respectively. Coefficients of variation for I_L and V_{OC} are much lower at 1.3% and 0.72%, respectively. Note that the observed maximum output power (P_{max}) for the modules (39.9 W median) is considerably less (14%) than the nameplate value (46.4 W).

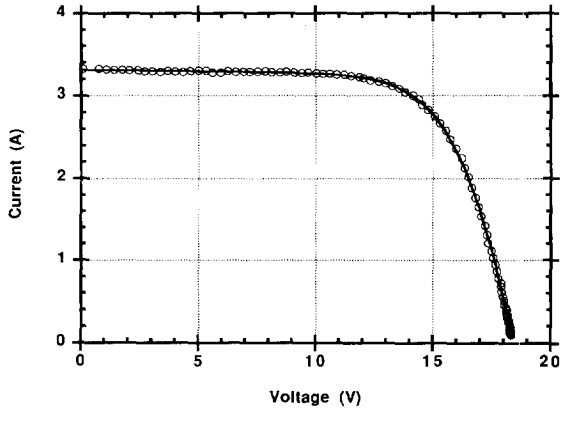

Fig. 1. Agreement between observed and estimated I–V curve using the five-parameter model.

Table 2. Variation of I–V curve parameters among modules at NOCT

Parameter	Units	Module mean	Module median	Module coefficient of variation (%)	Minimum	Maximum
P_{max}	W	39.8	39.9	2.1	37.5	42.4
I_L	A	3.29	3.29	1.3	3.17	3.47
V_{OC}	V	18.2	18.2	0.72	17.3	18.4
R_S	Ω	0.35	0.32	33.0	0.18	0.88
R_P	Ω	171.0	160.0	48.0	32.0	574.0
ekt	V^{-1}	0.71	0.68	18.0	0.56	1.72

Figures 2–6 present the cumulative distributions of the 192 estimates of I_L, V_{OC}, R_S, R_P, and *ekt* in normal probability plots. In these plots, data points that fall along a straight line can be described by a normal or Gaussian distribution function. Of the five, the distribution of I_L comes closest to being approximated by a normal distribution. All of the others substantially deviate from normality because they are skewed either positively (i.e., with a long tail toward high values) or negatively (i.e., with a long tail toward negative values).

Module parameters are also correlated with other module parameters, as summarized in Table 3. V_{OC} is statistically significantly correlated at the 5% significant level only with R_S, but all of the other parameters are statistically significantly correlated with each of the others. For example, modules with high values of R_S also generally would have high values of *ekt* and I_L and low values of R_P and V_{OC}.

3. VARIATION IN ARRAY PERFORMANCE

3.1 *Array models*

The effects of variation in module I–V curves, module orderings in arrays, and the array configuration on array performance were evaluated using a mathematical model of the array circuit. The two array configurations that have been investigated are shown in Fig. 7. Both contain four modules and result in an array open circuit voltage that is about two times the

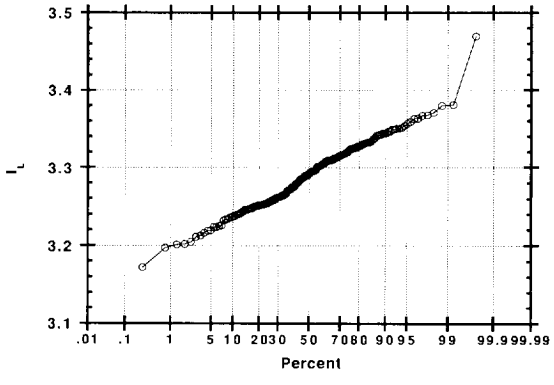

Fig. 2. Normal probability plot of module I_L parameter estimates.

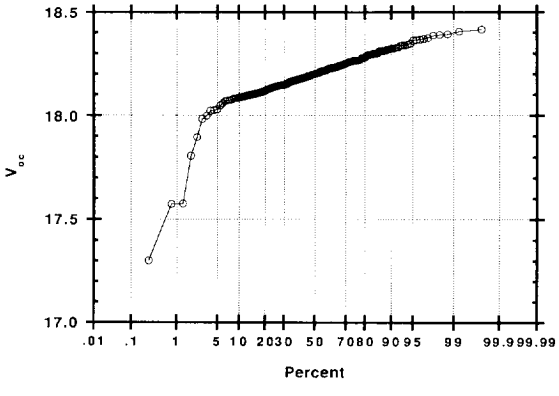

Fig. 3. Normal probability plot of module V_{OC} parameter estimates.

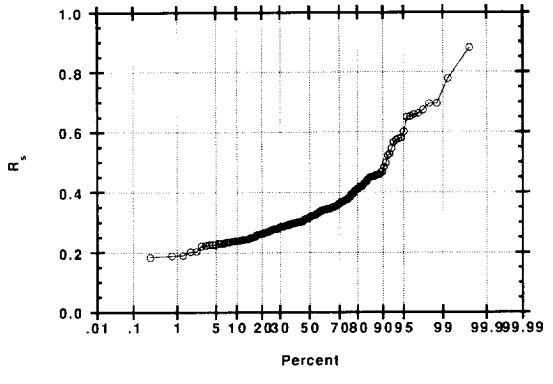

Fig. 4. Normal probability plot of module R_S parameter estimates.

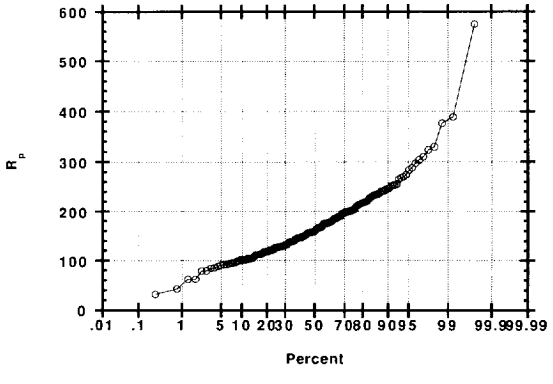

Fig. 5. Normal probability plot of module R_P parameter estimates.

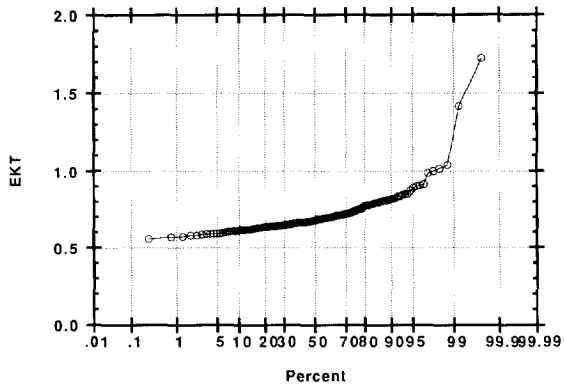

Fig. 6. Normal probability plot of module *ekt* parameter estimates.

Table 3. I–V curve parameter correlation matrix

	I_L	V_{OC}	R_S	R_P
V_{OC}	0.036			
R_S	0.187*	−0.215*		
R_P	−0.363*	−0.003	−0.390*	
ekt	0.144*	0.001	0.777*	−0.484*

* Statistically significant at the 5% significance level.

single module V_{OC} and in an array short circuit current that is about two times the single module V_{OC} and in an array short circuit current that is about two times the single module I_L. Following the terminology of Gonzalez and Weaver (1980), the two configurations are described as parallel strings and series blocks. These simple arrays were selected for study because Bucciarelli (1979) and Gonzalez and Weaver (1980) have shown that the mismatch losses are the greatest for such configurations.

In both configurations, the overall array voltage is V_T(V) and the overall array current is I_T(A). The I–V curve for each module (i, j) in the array is characterized by module-specific values for the five parameters $I_L(i, j)$, $V_{OC}(i, j)$, $R_S(i, j)$, $R_P(i, j)$, and $ekt(i, j)$. Using these module-specific parameters and the model given by eqn (1), the current $I_{i,j}$ produced by array module (i, j) at voltage $V_{i,j}$ can be expressed as:

$$I_{i,j} = f(V_{i,j}; I_L(i, j), V_{OC}(i, j), R_S(i, j), R_P(i, j), ekt(i, j)) \quad (5)$$

For each module it is also possible to express the module voltage $V_{i,j}$ as a function of module current $I_{i,j}$:

$$V_{i,j} = g(I_{i,j}; I_L(i, j), V_{OC}(i, j), R_S(i, j), R_P(i, j), ekt(i, j)) \quad (6)$$

For the parallel string configuration, the array current I_T produced at array voltage V_T can be determined by the solution of a system of nine simultaneous nonlinear equations for nine unknowns (I_T, $I_{1,1}$, $I_{2,1}$, $I_{1,2}$, $I_{2,2}$, $V_{1,1}$, $V_{2,1}$, $V_{1,2}$, $V_{2,2}$):

$$I_{1,1} - I_{2,1} = 0 \quad (7)$$

$$I_{1,2} - I_{2,2} = 0 \quad (8)$$

$$I_{1,1} + I_{1,2} - I_T = 0 \quad (9)$$

$$V_{1,1} + V_{2,1} - V_T = 0 \quad (10)$$

$$V_{1,2} + V_{2,2} - V_T = 0 \quad (11)$$

$$I_{1,1} = f(V_{1,1}; I_L(1,1), V_{OC}(1,1), R_S(1,1), R_P(1,1), ekt(1,1)) \quad (12)$$

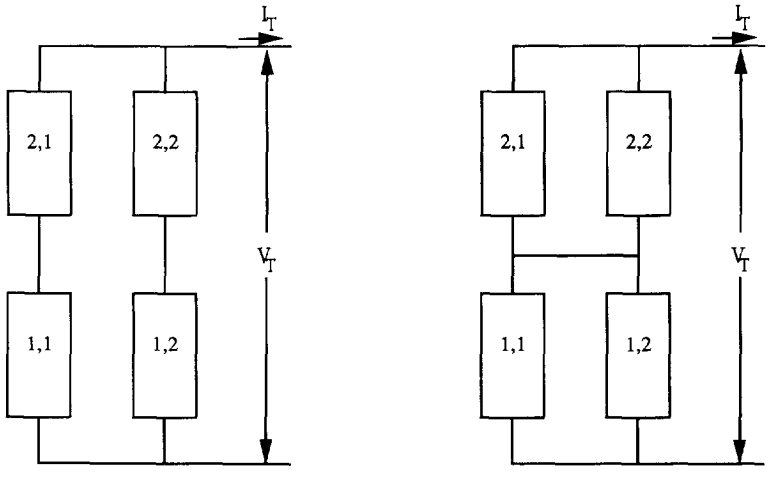

Series Strings Wired in Parallel (Parallel Strings) **Parallel Blocks in Series (Series Blocks)**

Fig. 7. Schematic diagram of parallel string and series block array configurations showing module indexing.

$$I_{1,2} = f(V_{1,2};\ I_L(1,2),\ V_{OC}(1,2),\ R_S(1,2),\ R_P(1,2),\ ekt(1,2)) \quad (13)$$

$$I_{2,1} = f(V_{2,1};\ I_L(2,1),\ V_{OC}(2,1),\ R_S(2,1),\ R_P(2,1),\ ekt(2,1)) \quad (14)$$

$$I_{2,2} = f(V_{2,2};\ I_L(2,2),\ V_{OC}(2,2),\ R_S(2,2),\ R_P(2,2),\ ekt(2,2)) \quad (15)$$

For the series block configuration, the array voltage V_T produced at array current I_T can also be determined by the solution of a system of nine simultaneous nonlinear equations for nine unknowns (V_T, $I_{1,1}$, $I_{2,1}$, $I_{1,2}$, $I_{2,2}$, $V_{1,1}$, $V_{2,1}$, $V_{1,2}$, $V_{2,2}$):

$$I_{1,1} + I_{1,2} - I_T = 0 \quad (16)$$

$$I_{2,1} + I_{2,2} - I_T = 0 \quad (17)$$

$$V_{1,1} + V_{2,1} - V_T = 0 \quad (18)$$

$$V_{1,1} - V_{1,2} = 0 \quad (19)$$

$$V_{2,1} - V_{2,2} = 0 \quad (20)$$

$$V_{1,1} = g(I_{1,1};\ I_L(1,1),\ V_{OC}(1,1),\ R_S(1,1),\ R_P(1,1),\ ekt(1,1)) \quad (21)$$

$$V_{1,2} = g(I_{1,2};\ I_L(1,2),\ V_{OC}(1,2),\ R_S(1,2),\ R_P(1,2),\ ekt(1,2)) \quad (22)$$

$$V_{2,1} = g(I_{2,1};\ I_L(2,1),\ V_{OC}(2,1),\ R_S(2,1),\ R_P(2,1),\ ekt(2,1)) \quad (23)$$

$$V_{2,2} = g(I_{2,2};\ I_L(2,2),\ V_{OC}(2,2),\ R_S(2,2),\ R_P(2,2),\ ekt(2,2)) \quad (24)$$

3.2 *Distribution of array power*

The 192 modules tested were randomly selected and arranged into 200 four-module sets. This random subsampling provided modules that exhibited the observed variation in module characteristics, including the correlation among module parameters. Each of these sets was configured as both a parallel string and a series block array. Neglecting module position within the array, over $50 \cdot 10^6$ distinct four-module arrays can be created from the 192 modules. The maximum output power, P_{max} (W), for each array configuration was calculated using the parameter estimates available for each module and the appropriate array model presented above. Using the calculated I–V curve for each array configuration, the output power was calculated at 0.01 V intervals until the maximum was determined.

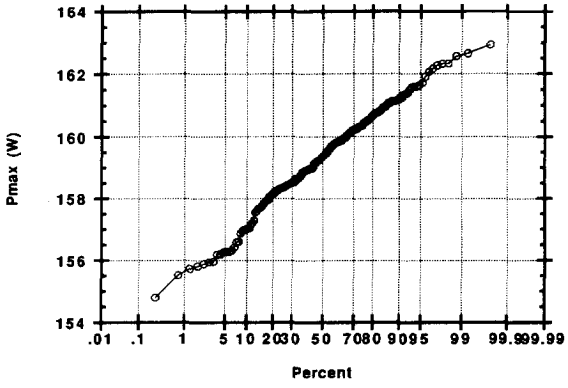

Fig. 8. Normal probability plot of maximum output power (P_{max}) from parallel string array.

Figures 8 and 9 show the cumulative distributions of P_{max} for the parallel string and series block array configurations, respectively. These two distributions are indistinguishable at the 5% significance level based on the Kolmogorov–Smirnov test as described by Benjamin and Cornell (1970). Table 4 summarizes the statistical characteristics of the maximum output power produced by the random module arrays in the parallel string and series block configurations. Clearly, the statistical properties of P_{max} are very similar for the two configurations.

Figure 10 compares the maximum output power from the parallel string and the series blocks arrays and shows that the maximum output power does not depend on the array configuration but only on the modules selected. Table 4 provides a summary of the difference in maximum output power (ΔP_{max}) produced by the parallel string and series block arrays for each of the 200 sets of four randomly selected modules. The median and mean difference in P_{max} was only 0.01 W and ranged from −0.52 W to 0.60 W relative to the median value of P_{max} of 159 W.

The percent mismatch loss (MML) for each array was calculated based on the total of the maximum output power from each of the modules in the array and the calculated maximum output power of the array (P_{max}):

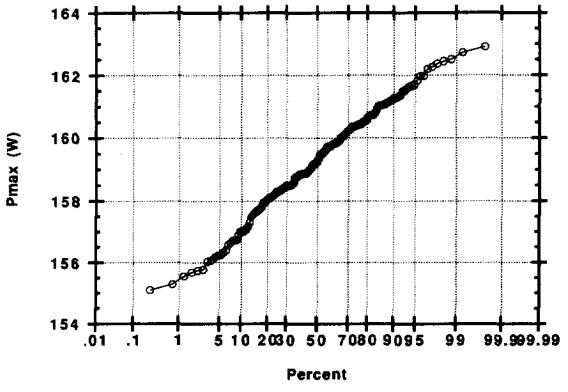

Fig. 9. Normal probability plot of maximum output power (P_{max}) from series block array.

Table 4. General tendency and variation in maximum output power and mismatch loss in random module parallel string and series block arrays

Variable	Minimum	Maximum	Median	Mean	Standard deviation
P_{max} without mistmatch (W)	155.27	162.94	159.47	159.40	1.6
Parallel string P_{max} (W)	154.76	162.87	159.30	159.26	1.6
Series block P_{max} (W)	155.07	162.88	159.26	159.24	1.6
ΔP_{max} (W)*	−0.52	0.60	0.01	0.01	0.14
Parallel string mismatch loss (%)	−0.00	0.53	0.06	0.08	0.08
Series block mismatch loss (%)	0.01	0.45	0.07	0.09	0.08

* $\Delta P_{max} = P_{max}$(parallel string) $- P_{max}$(series block).

$$\mathrm{MML} = \frac{\left(\sum_{i=1}^{2}\sum_{j=1}^{2} \max(I_{i,j} \cdot V_{i,j}) - P_{max}\right) \cdot 100}{\sum_{i=1}^{2}\sum_{j=1}^{2} \max(I_{i,j} \cdot V_{i,j})} \quad (25)$$

Table 4 summarizes the observed percent mismatch losses for the two array configurations. The largest percent mismatch loss was only 0.53% and the mean values were less than 0.1%. Figure 11 presents the cumulative distribution of mismatch loss for each array configuration.

4. DISCUSSION

The five-parameter I–V curve model, eqn (1), provides an accurate basis for predicting module response and also provides precise estimates of the module I–V curve parameters: I_L, V_{OC}, R_S, R_P, and *ekt*. Module-to-module variation in the I–V curve parameters was more than 10 times greater than the uncertainty in the corresponding module estimates. For example, the estimates of V_{OC} had a median coefficient of variation of 0.04%, while the coefficient for module-to-module variation in V_{OC} was 0.72% which is 18 times greater. Consequently, the uncertainty in the module parameter estimates does not substantially obscure the variation from module-to-module.

The maximum output power at NOCT for the modules ranged from 37.5 W to 42.4 W with a coefficient of variation of 2.1%. I_L ranged from 3.17 A to 3.47 A with a coefficient of variation of 1.3%. This variation is considerably less than that assumed by Bucciarelli (1979) and Gonzalez and Weaver (1980) in their analyses of mismatch losses.

The discrepancy between the nameplate ratings of the modules tested and the observed maximum out power at NOCT may be in part explained by the variation in the spectral characteristics of the natural insolation during the field tests and by other deviations in testing conditions. But the 14% average difference observed is consistent with the 5–13% discrepancy reported by Jennings (1987) and the 9% discrepancy reported by Russell and Bergman (1985).

As with the individual modules, the maximum output power from the four module arrays was 14% (27 W) less than would be expected from the nameplate ratings: 159 W versus 186 W. But the coefficient of variation in maximum output power in the random module arrays was only 1.0% or 1.6 W with the range in maximum output power only from 155 W to 163 W.

No substantial difference in maximum output power or mismatch losses between the parallel string and series block array configurations was observed. This contradicts Green (1982) and Gonzalez and Weaver (1980) who concluded that series block configurations should exhibit less severe mismatch losses than parallel strings. However, the earlier work focused primarily on cell-to-cell variation within a module rather than module-to-module variation within an

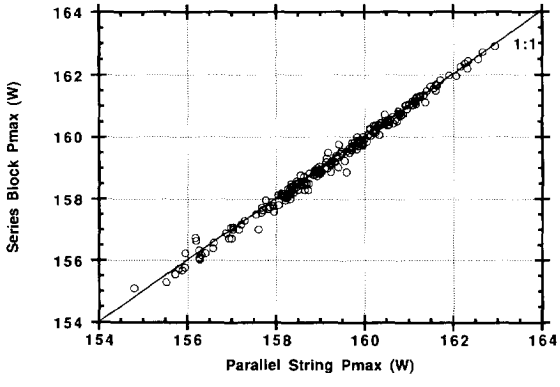

Fig. 10. Relationship between maximum power output (P_{max}) from parallel string and series block arrays. Line shown represents equal maximum output power from the two array configurations.

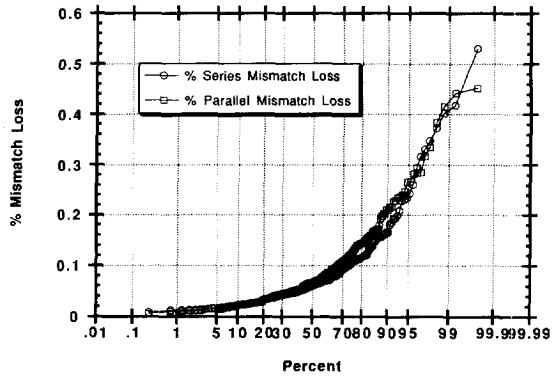

Fig. 11. Normal probability plot of mismatch loss from parallel string and series block arrays.

array and addressed more substantial differences in cell (or module) characteristics.

Based on this investigation, arrays composed of undamaged production-run modules of a single model and manufacturer do not exhibit significant mismatch losses. The discrepancies between actual and expected array performance are overwhelmingly the result of deviations from the nameplate ratings. No significant gains in array performance can be obtained by use of series block versus parallel string configurations, or by selective ordering of modules within the array.

This investigation has not considered the effect of inclusion of damaged modules, modules operating at substantially different temperature or insolation, or different kinds of modules within arrays. Under such conditions, array configuration and module ordering may yield substantial gains in performance.

5. CONCLUSIONS

1. The five-parameter I–V curve model given by eqn (1) provides an accurate basis for predicting module response and also provides precise estimates of the module I–V curve parameters: I_L, V_{OC}, R_S, R_P, and ekt.
2. The 192 production-run ARCO Solar M75 Solar Electric Modules exhibited small variation in P_{max}, I_L, and V_{OC} with coefficients of variation of 2.1%, 1.3%, and 0.72%, respectively. The modules showed much higher variation in R_S, R_P, and ekt with coefficients of variation of 33%, 48%, and 18%, respectively. Most module parameters were statistically significantly correlated with other parameters.
3. The observed maximum output power from the modules averaged 14% less than the nameplate rating at NOCT.
4. No discernible difference was observed in the maximum output power from parallel string arrays and series block arrays.
5. Mismatch losses were very small, averaging 0.1% and always less than 0.53%.
6. Consideration of mismatch losses is unwarranted in the design of arrays composed of undamaged, production-run modules of a single model operating at a uniform temperature and insolation.

Acknowledgment—The authors gratefully acknowledge the generous project funding provided by Mr. L. W. Schatz of General Plastics Manufacturing Co., Tacoma, WA, U.S.A.

REFERENCES

Y. Bard, Nonlinear parameter estimation and programming, IBM Cambridge Scientific Center, Cambridge, MA (1967).

J. R. Benjamin and C. A. Cornell, Probability, statistics, and decision for civil engineers, McGraw-Hill, New York (1970).

L. Bucciarelli, Jr., Power loss in photovoltaic arrays due to mismatch in cell characteristics, *Solar Energy*, **23**, 277–288 (1979).

R. Engle, Amorphous silicon solar module performance at low insolation levels, Senior Project, Environmental Resources Engineering, Humboldt State University, (1988).

C. Gonzalez and R. Weaver, Circuit design considerations for photovoltaic modules and systems, 14th IEEE Photovoltaics Specialists Conference, San Diego, CA (1980).

M. A. Green, Solar cells-operating principles, technology, and system applications, Prentice-Hall, Englewood Cliffs, New Jersey (1982).

C. Jennings, Outdoor versus rated photovoltaic module performance, 19th IEEE Photovoltaic Specialists Conference, New Orleans, LA (1987).

P. Lehman and C. E. Chamberlin, Field measurements of flat-plate module performance in Humboldt County, California, 19th IEEE Photovoltaic Specialists Conference, New Orleans, LA (1987).

M. C. Russell and D. A. Bergman, Photovoltaic flat-plate array and insolation measurements, Proc. Photovoltaics and Insolation Measurements Workshop, Vail, Colorado, Solar Energy Research Institute, Golden, Colorado (1985).